

Optimized Operational Cost Reduction for an EV Charging Station Integrated With Battery Energy Storage and PV Generation

Qin Yan ¹, *Student Member, IEEE*, Bei Zhang, *Student Member, IEEE*, and Mladen Kezunovic, *Life Fellow, IEEE*

Abstract—A four-stage intelligent optimization and control algorithm for an electric vehicle (EV) bidirectional charging station equipped with photovoltaic generation and fixed battery energy storage and integrated with a commercial building is proposed in this paper. The proposed algorithm aims at maximally reducing the customer satisfaction-involved operational cost considering the potential uncertainties, while balancing the real-time supply and demand by adjusting the optimally scheduled charging/discharging of EV mobile/local battery storage, grid supply, and deferrable load. The chance-constrained optimization objective has been stated in stages: 1) stage I, optimization of day-ahead energy management schedules; 2) stage II, multitiered EV charging price update and optimization of discharging participation bonus; 3) stage III, optimization of hour-ahead energy management schedules; and 4) stage IV, real-time control. Such algorithm provides more resilience for unpredictable conditions, provides more incentives for EV users to participate, and better coordinates the integrated system including the building load to reliably serve the customers while lessening cost. Case studies are implemented and the comparison analysis is performed in terms of the use and benefit of each design feature of the algorithm. The results indicate that the proposed algorithm can reduce the operational cost and at the same time provide higher tolerability toward uncertainties.

Index Terms—Plug-in electric vehicle (PEV), optimization and control algorithm, charging station, photovoltaic (PV) generation, battery storage, commercial building.

NOMENCLATURE

t, T	Index of time, total number of time slots
b_b^t	Electricity consumption of building b connected to the charging station
$e_i^{t+}, e_i^{t-}, e_i^t$	Amount of i -th PEV's power that is charged (+) or discharged (−), and $e_i^t = e_i^{t+} - e_i^{t-}$
p_{PV}^t	Power that the PV generation can provide
$P_G^{t+}, P_G^{t-}, P_G^t$	Power transaction from (+) or to main grid (−), and $P_G^t = P_G^{t+} - P_G^{t-}$

σ_G, σ_{EV}	Unit bonus for supplying power back to grid/discharging of the participating PEVs
$\theta_{EV}, \theta_{PV}, \theta_{BS}$	Unit cost for charging PEVs/ operating PVs/ operating battery storages
σ	Electricity price, unit cost of the power supplied by grid
c_b^{EENS}	Unit cost for energy not supplied (EENS) for building b , with different load types
D_b^t, b_b^t	Load demand/ actual load supplied for building b
e_i^{\max}	Battery capacity of PEV i
SOC_i^{in}, SOC_i^{fn}	Initial and pre-determined target SOC for PEV i
T_i^0, T_i	Time when PEV i starts to connect and total connection time
$e_i^{\max,d}, e_i^{\max,c}$	Maximum allowable discharging/ charging rate for PEV i
b_b^{\max}	Maximum allowable demand of building b
P_{PV}^{\max}	Capacity of PV
$s_{BS}^{\max,d}, s_{BS}^{\max,c}$	Maximum allowable discharging/ charging rate for battery storage
$s_{BS}^{t+}, s_{BS}^{t-}, s_{BS}^t$	Amount of battery storage power that is charged (+) or discharged (−), $s_{BS}^t = s_{BS}^{t+} - s_{BS}^{t-}$
s_{BS}^{\max}	Capacity of battery storage
P_{cs}^{\max}	Power flow limit for the integrated charging station
$E_{EV,total}^t$	Total energy need from PEVs in the charging station at time t
$b_{b,j}^t$	j th type of energy need from the building b at time t
ω	Corresponding standard deviations
$R_{ei}^{b,k}$	Assumed reliability for supplying the load of the k th priority
Ω	Set of the faults to be considered
J_b	Number of classified building load.

Manuscript received July 13, 2017; revised October 12, 2017 and November 17, 2017; accepted December 24, 2017. Date of publication January 1, 2018; date of current version February 18, 2019. This publication was made possible by NPRP 8-241-2-095 from the Qatar National Research Fund (a member of Qatar Foundation). The statements made herein are solely the responsibility of the authors. Paper no. TSG-00977-2017. (*Corresponding author: Qin Yan.*)

The authors are with the Department of Electrical and Computer Engineering, Texas A&M University, College Station, TX 77840 USA (e-mail: judyqinyan2010@tamu.edu).

Color versions of one or more of the figures in this paper are available online at <http://ieeexplore.ieee.org>.

Digital Object Identifier 10.1109/TSG.2017.2788440

I. INTRODUCTION

RENEWABLE generation and transportation electrification utilization are emerging as the most promising strategies to meet the increasing environmental concerns and energy scarcity, and this trend is expected to grow in the future [1]. Statistically, more than 90% of the time on average passenger vehicles are parked and their idle time is much

longer than the required time to fully recharge the batteries [2]. Plug-in Electric Vehicles (PEVs) equipped with batteries are estimated to be idle the same length of time as a utility generator is used for an on-line operation [1], [2]. Thus, as an environmentally and economically friendly choice for transportation, PEVs can be used both as a mobile energy storage, and as a generator to support buildings' energy demand [3].

Furthermore, 30% of the end-use energy-related carbon emission is from load consumption of buildings including commercial and residential ones, which consume about 32% of the total global energy use [4]. As such, PEVs are considered to help increase reliability of power supply and reduce energy cost with demand side management via vehicle-to-building (V2B) operation mode [5]–[8]. Roof-top PV generation is also considered as an efficient way to meet the buildings energy demand [9], [10].

The renewable energy resources such as solar, being naturally abundant in some regions and clean, are important component to provide ancillary energy. Many researches integrated PEV charging stations with PV generation to help lower the cost as well as reduce the carbon footprint [11]–[14]. To address the random nature of renewable energy, additional storage or spinning reserve are often utilized [15]–[17].

To deal with the intermittent and variable properties of the renewable energy resources, many optimization or control algorithms are proposed [18]–[22], including ordinal optimization [18], genetic algorithm [19], and model-predictive control approach [2], [13], [22]. But, not all the factors such as operational cost, customer satisfaction, load loss, and profit for charging station owners are considered in one objective function. For example, only PEV charging cost as a convex function of load demand is considered to be minimized in [22]. Some papers classified PEVs by the owners' preference [11], but none of the papers classifies PEVs based on real-time state and charging demand. Although a lot of work aimed at reducing the complexity of the optimization algorithm to coordinate the PEV charging, i.e., by sacrificing minimum performance gap, still substantial time is required to compute and obtain the optimal results. The recent work reported in [22] indicates that the computational complexity is $O(T^3)$ and the computational time for each stage has the range of 1-10 seconds for each PEV. The computational time needs to be reduced to realize the real-time coordination.

In this paper, we separate the stages into ahead-of-time optimal scheduling and real-time control. A novel four-stage optimization and control algorithm is proposed targeting reduction in total operating cost for a charging station integrated with PV, fixed battery storage and a commercial building. Day-ahead and hour-ahead predictive data are used and model predictive control-based method is utilized for those predicted data. Operating cost optimization model is established considering the potential uncertainties and customer satisfaction indices. Load is classified by the significance and flexibility. EV discharging is encouraged by adding and maximizing the participation bonus. Thus, such algorithm can attract more EV customers to participate in discharging program, provide more resilience in face of unpredictable

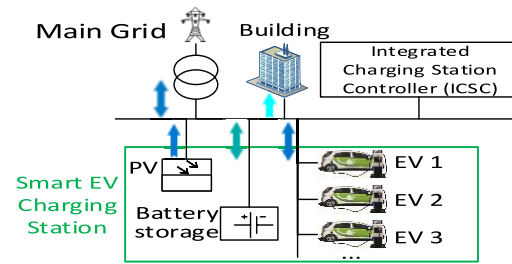


Fig. 1. Network of integrated smart charging stations.

circumstances, and more reliably serve the customers by coordinating both supply and demand.

The rest of the paper is organized as follows: Section II describes the framework of the proposed four-stage optimization and control algorithm with scenario definitions, optimization model, control strategy, and the evaluation methods explained in detail in related subsections. In Section III, case studies are described and the assigned values for related parameters are given. In addition, test case comparisons are conducted, results are analyzed and conclusions are made. Contributions of the paper are outlined in Section IV followed by references.

II. FOUR-STAGE OPTIMIZATION AND CONTROL ALGORITHM

An integrated smart charging station as shown in Fig. 1 is considered. Building is connected to the same bus as the integrated charging station components, namely PV panels, and fixed battery storage. The PEVs are assumed to support both the charging and discharging mode. Fixed battery storage also operates in the two modes as needed. The output power of PV generation is strongly affected by ambient weather conditions. The integrated charging station considered in this paper is assumed to be located in the parking lots inside or close to the commercial building. It is rational and beneficial to supply the load demand of the building when the integrated charging station has more power supply available, instead of directly injecting power back to the grid. It will be better if the imbalance between the supply and demand can be self-digested. Thus, in this paper, the building is integrated with the charging station, and the load of the building is considered as a “responsibility” for the integrated charging station. Therefore, the load of the building is directly supplied by the integrated charging station. The profit or the load loss cost will also be attributed to the charging station owner.

In order to coordinate the operation of the integrated charging station, an optimization and control algorithm is required. The real-time control algorithm is based on the optimization results. To be more accurate in the optimization schedules and to consider the unexpected occurrence on that day, hour-ahead forecast data is used in addition to day-ahead forecast data before each hour. Since the day-ahead optimal schedules of battery charging/discharging will change the power demand profile, the EV charging prices for each hour can be updated to track the demand change, and participation bonus for EV discharging can be updated to satisfy EV owners to the

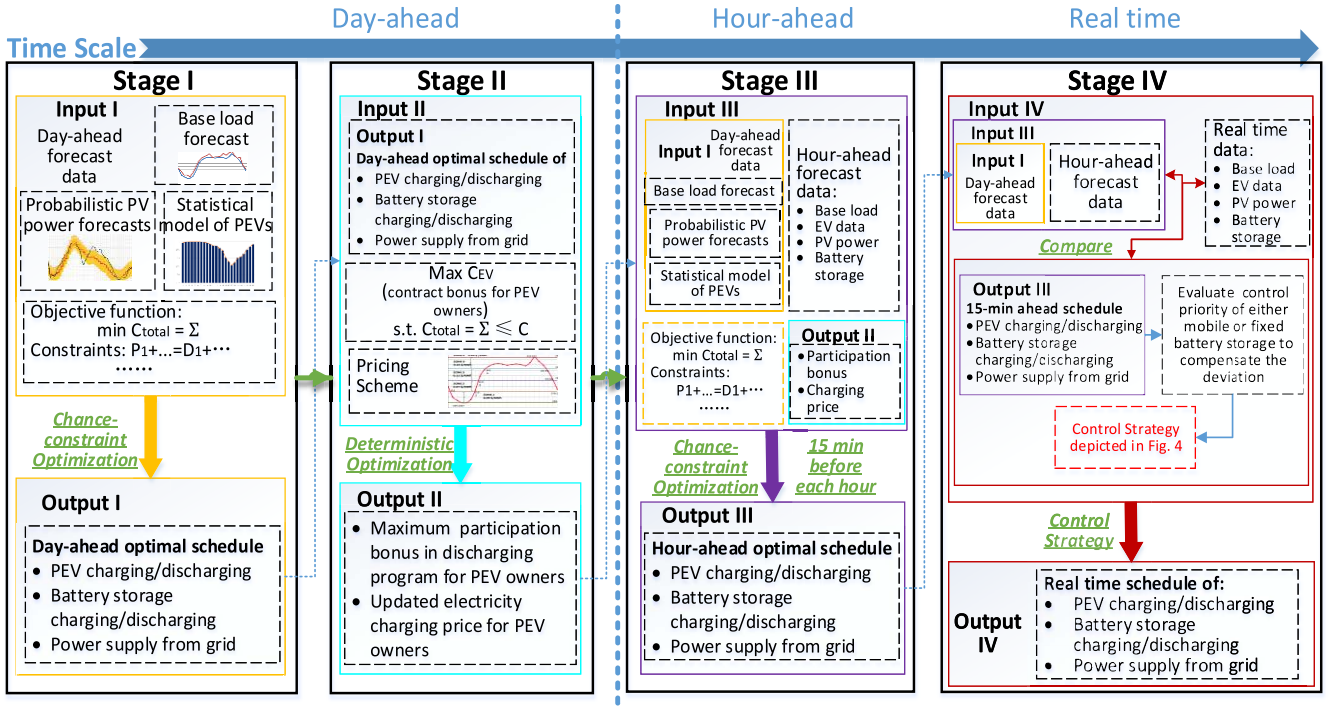


Fig. 2. Four-stage optimization and control algorithm.

greatest extent and at the same time meet charging station's requirement. The advantages of each stage are further evaluated and analyzed in Section III. Thus, a four-stage operational cost reduction algorithm described by the flowchart shown in Fig. 2 is proposed.

Chance-constrained optimization is utilized in stage I and stage III, aiming at supplying the building energy need by the integrated charging station in a more reliable way considering various uncertainties. According to the load demand on-peak and off-peak hours, the result from stage I is used in stage II to obtain new charging price based on [23] and maximum participation bonus to attract PEV customers to be involved in charging/discharging program for the next day, as well as to guarantee a specific maximum cost boundary. To make it a better reference for the real-time operation, stage III optimization considering hour-ahead forecast data with prices obtained in stage II, is implemented every hour, i.e., 15 minutes before each hour. Each simulation covers the hours from the start of next hour to the last departure time of the predicted PEV participant. To manage the difference between predicted and real data, real-time control aimed at adjusting the hour-ahead schedules is implemented in stage IV.

The highlight of the four-stage algorithm lies in the design of the timeline spanning three time scales, an additional stage to maximize the participation bonus for PEV discharging, and the use of proposed control scheme. In short, the models used for stage I and III are formulated in the following Section II-B; the pricing scheme used to update charging price and discharging participation bonus is elaborated in [23] and Fig. 2; and the logic flowchart of the control strategy are depicted in Fig. 4 and the following Section II-C.

A. Scenario Description and Definition

Generally speaking, one day (24 hours) is regarded as a whole simulation cycle. However, the last PEV to stay in the charging station is usually staying past midnight. Thus, in the proposed algorithm, simulation cycle for a day is still 24 hours long (starts at midnight), but the coverage time in each simulation is not necessarily 24 hours but determined by the departure time of the PEV which is the last one to leave.

The day-ahead forecast for PEV itineraries is based on the statistical analysis of PEV electricity consumption discussed in [24]. Let $e_i^{T_i^0}$ be the battery energy level when PEV i starts to connect at T_i^0 , and E_i be the pre-determined target of battery energy level when disconnected. Then the energy transfer of each PEV i over the total connection time T_i should satisfy,

$$\begin{aligned} \sum_{t=T_i^0+1}^{T_i^0+T_i} e_i^t &= \sum_{t=T_i^0+1}^{T_i^0+T_i} (e_i^{t+} - e_i^{t-}) = E_i - e_i^{T_i^0} \\ &= SOC_i^{fn} \times e_i^{\max} - SOC_i^{in} \times e_i^{\max} \end{aligned} \quad (1)$$

The load is classified into four types: critical load, power-controllable load, deferrable load and less important load. The power required by essential appliances are regarded as critical load. Such load has to be always supplied. Power-controllable load can be some flexible appliances such as thermostat load (air conditioner or water heater), which is required but can be controlled. Deferrable load requires power for a certain but shiftable duration, such as laundry machines or dishwashers. The remaining optional load is treated as less important load. The percentage of the load demand for each type is estimated based on references [25]–[27], as shown in Fig. 3. The base load for a building is estimated based on the real load profile

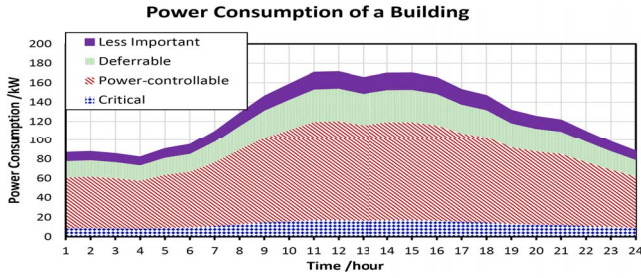


Fig. 3. Power Consumption of a Building.

data from New Hampshire Electric Co-op (NHEC) [28]. The cost of expected energy not supplied (EENS) indices for each load type are determined referring to [29].

B. Optimization Model

The improvement on the optimal planning scheme for scheduling the operation of the charging station lies in the classification of different load types, customer satisfaction indices reflected in the cost function, ability to provide bidirectional power flow with main grid, the impact of the operation of the charging station on the node voltage, etc.

The objective function of the optimization model involves cost of power supplied by the grid, operating cost of PV and fixed battery storage, cost of unsupplied demand, cost of discharging PEVs and profits from charging PEVs and providing power back to the grid.

In (2), as shown at the bottom of this page, where $C_b^{EENS,t}$ can be expressed in (3) if several buildings are connected to the charging station.

$$\begin{aligned} C_b^{EENS,t} &= \sum_{b_1} C_{b_1}^{EENS,t} + \sum_{b_2} C_{b_2}^{EENS,t} + \dots \\ &= \sum_{b_1} \left((D_{b_1}^t - b_{b_1}^t) \times c_{b_1}^{EENS} \right) \\ &\quad + \sum_{b_2} \left((D_{b_2}^t - b_{b_2}^t) \times c_{b_2}^{EENS} \right) + \dots \quad (3) \end{aligned}$$

Constraints: $\forall t = 1, \dots, T$

- For each building b :

$$0 \leq b_b^t \leq b_b^{\max} \quad (4)$$

- For each PEV i :

$$\begin{cases} 0 \leq e_i^{t+} \leq e_i^{\max,c}, t \in [T_i^0, T_i^0 + T_i] \\ 0 \leq e_i^{t-} \leq e_i^{\max,d}, t \in [T_i^0, T_i^0 + T_i] \\ 20\% \times e_i^{\max} \leq e_i^{T_i^0} + \sum_0^t e_i^t \leq e_i^{\max} \\ \begin{cases} e_i^{T_i^0} = SOC_i^{in} \times e_i^{\max} \\ \sum_{t=T_i^0+1}^{T_i^0+T_i} e_i^t = SOC_i^{fn} \times e_i^{\max} - e_i^{T_i^0} \end{cases} \end{cases} \quad (5)$$

At any time, the energy in each PEV cannot be negative nor exceed the battery capacity. In addition, the number of connected PEVs should be less than the number of chargers.

- For PV:

$$0 \leq p_{PV}^t \leq p_{PV}^{\max} \quad (6)$$

- For each battery storage,

$$\begin{cases} -s_{BS}^{\max,d} \leq s_{BS}^t \leq s_{BS}^{\max,c} \\ 0 \leq \sum_0^t s_{BS}^t \leq s_{BS}^{\max} \end{cases} \quad (7)$$

- Power constraints:

$$\sum_i e_i^t + b_b^t = p_{PV}^t + s_{BS}^t + P_G^t \quad (8)$$

- Power flow equations for each bus l :

$$\begin{aligned} P_{G_l}^t + \sum_{j \in l} p_{PV,j}^t + \sum_{n \in l} s_{BS,n}^t - \sum_{i \in l} e_i^t - \sum_{b \in l} b_b^t - P_{D_l}^t \\ = V_l^t \sum_{x=1}^{n_l} V_x^t (G_{lx} \cos \delta_{lx} + B_{lx} \sin \delta_{lx}) \quad (9) \end{aligned}$$

- Power flow constraints for integrated charging station:

$$-P_{cs}^{\max} \leq \sum_i e_i^t + b_b^t - p_{PV}^t - s_{BS}^t = P_G^t \leq P_{cs}^{\max} \quad (10)$$

$$\begin{aligned} \text{total cost} \\ \text{Min } \overbrace{C_{total}^t} &= \sum_t \left(\begin{array}{cccc} \text{cost of power supplied by grid} & \text{contract with participating PEVs} & \text{operating cost of PV} & \text{cost of unsupplied demand (EVs \& building)} \\ \underbrace{C_G^t} & + \sum_i \underbrace{C_{c,i}^t} & + \underbrace{C_{PV}^t} & + \underbrace{C_b^{EENS,t}} \\ \\ \text{operating cost of storage} & \text{profit from charging PEVs} & \text{profit from supplying grid} & \\ + \underbrace{C_{BS}^t} & - \sum_i \underbrace{Pr_i^t} & - \underbrace{Pr_G^t} & \end{array} \right) \\ &= \left(\begin{array}{cccc} \text{cost of power supplied by grid} & \text{contract with participating PEV} & \text{operating cost of PV} & \\ \sum_t (\sigma \times P_G^{t+}) & + \sum_t \sum_i (\sigma_{EV} \times e_i^{t-}) & + \theta_{PV} \times p_{PV}^{\max} & \\ \\ \text{cost of unsupplied customers} & \text{operating cost of storage} & \text{profit from charging PEV} & \text{profit from supplying grid} \\ + \sum_t (D_b^t - b_b^t) \times c_b^{EENS} & + \theta_{BS} \times s_{BS}^{\max} & - \sum_i \left(\theta_{EV} \times \sum_t e_i^{t+} \right) & - \sum_t (\sigma_G \times P_G^{t-}) \end{array} \right) \quad (2) \end{aligned}$$

- Voltage constraint:

$$V_l^{\min} \leq V_l^t \leq V_l^{\max} \quad (11)$$

- Bus constraints:

$$\begin{cases} -P_{G_l}^{\max} \leq P_{G_l}^t \leq P_{G_l}^{\max} \\ -Q_{G_l}^{\max} \leq Q_{G_l}^t \leq Q_{G_l}^{\max} \\ \sum_x P_{lx}^t = P_{G_l}^t + \sum_{j \in l} P_{PV,j}^t + \sum_{n \in l} S_{BS,n}^t - \sum_{i \in l} e_i^t \\ \quad - \sum_{b \in l} b_{b,j}^t - P_{D_l}^t \\ \sum_x Q_{lx}^t = Q_{G_l}^t - Q_{D_l}^t \\ \begin{cases} P_{xl}^t = -P_{lx}^t \\ Q_{xl}^t = -Q_{lx}^t \end{cases} \\ \begin{cases} -P_{lx}^{-\max} \leq P_{lx}^t \leq P_{lx}^{\max} \\ -Q_{lx}^{-\max} \leq Q_{lx}^t \leq Q_{lx}^{\max} \end{cases} \end{cases} \quad (12)$$

where l indicates the bus to which the integrated charging station is connected. P_{G_l} and P_{D_l} include all the generators and loads connected to the same bus l . x represents all the adjacent buses if a complete power network is considered.

1) *Chance-Constrained Optimization*: Different from the deterministic optimization, the chance constrained optimization is trying to consider the uncertainties behind the parameters. Those uncertainties are usually modeled by probability distributions, and the deterministic constraints $\mathbf{Ax} \geq \mathbf{b}$ can be replaced by the chance-constrained constraints that the probability that $\mathbf{Ax} \geq \mathbf{b}$ can be satisfied is higher/lower than a certain chance.

To more reliably serve the PEV owners and back up the energy supply to the building, chance-constrained optimization is adopted to handle the following uncertainties: hourly charging need for the charging station, PV generation, the energy need by the building, and the power supply from the grid under fault i , as modeled in (13-15). Uncertainty also exists in the power supply from the grid side, since it may be interrupted when a fault happens. We assume that the probability of the fault i is P_{rob_fi} , and the power supply from the grid under fault i is modeled in (16), where $P_{G,fi}^t$ is the possible available power from the grid under fault i at time t .

$$E_{EV,total}^t \sim E(E_{EV,total}^t) + N(0, \omega_{EV,total,t}^2) \quad (13)$$

$$P_{PV}^t \sim E(p_{PV}^t) + N(0, \omega_{PV,t}^2) \quad (14)$$

$$b_{b,j}^t \sim E(b_{b,j}^t) + N(0, \omega_{b,j,t}^2) \quad (15)$$

$$P_{G,fi}^t \sim E(P_{G,fi}^t) + N(0, \omega_{G,t,fi}^2) \quad (16)$$

Our aim is to make sure the sustainable energy supply for the important demand from both PEV customers and building customers. Equation (17) tries to set the probability of the sustainable supply to be higher than R_{ei} under fault f_i at time t_{fi} , assuming that the fault is going to last for T_{fi} .

$$\begin{aligned} & P_{rob}^{t,fi} \left(\sum_0^t s_{BS}^t + \sum_{t=t_{fi}}^{t_{fi}+T_{fi}} p_{PV}^t + \sum_{t=t_{fi}}^{t_{fi}+T_{fi}} P_{G,fi}^t \geq \sum_{j=1}^k \sum_{t=t_{fi}}^{t_{fi}+T_{fi}} load_j^t \right) \\ & \geq 1 - \frac{1 - R_{ei}^{b,k}}{P_{rob_fi}}, t = 1, 2, \dots, T, fi \in \Omega, k = 1, 2, \dots, J_b \end{aligned} \quad (17)$$

Energy need from the building and PEV charging needs to be classified and prioritized based on the consequence of energy not supplied. Note that the PEV charging need is also prioritized along with the building load, and $load_j^t$ is the combined classification result of both $b_{b,j}^t$ and $E_{EV,total}^t$.

This optimization model aims at minimizing the overall operational cost for each element in the integrated system. This method allows PV to generate as much power as possible. Due to the charging/discharging efficiency of batteries, fixed battery storage is not the preferable source of power if other power source is available, such as PV or power grid based on the prices. The customer satisfaction indices determine that the load loss is the least wanted situation. The relationship between the electricity price, charging price and discharging participation price for EVs determines the optimal schedule of EV charging/discharging and power supply needed from the main grid. Indeed, the optimal solution obtained in stage I will not be optimal once the prices are updated in stage II. That leads to the necessity of stage III to have new hour-ahead input and new prices for the hour-ahead optimization solution.

Note that, in this work, to save more computational time and simplify the simulation work, the optimization model is solved as DC system. The nonlinear power flow equation (9) is used to calculate voltage and equation (11) is checked to see if the voltage constraint is satisfied. If the constraint is not satisfied, the obtained optimal results will be excluded and optimization will be performed again.

After obtaining day-ahead optimization solution in stage I, new charging price is obtained by utilizing the pricing scheme stated in reference [23] in stage II. The multi-tiered electric pricing scheme divided the load profile into five zones and assigned different charging price for each zone. Since the load profile will change after applying the optimization solution from stage I, the charging price also needs to be updated accordingly.

C. Control Strategy

The highlight of the control scheme lies in the different scenarios differentiated by comparison results, classification of PEV groups and the logic to optimize each schedule in terms of prediction deviation, etc.

The flowchart of the control scheme is shown in Fig. 4 with the input data included in the red box on the left hand side. The value of Dif indicates whether more power supply is available or more demand is needed in real time. The control process differs based on Dif , electricity price, c_b^{EENS} , etc.

These divide the control scheme into four scenarios, in which the checking sequences are different. The underlying principles are as follow:

- Output power from PV is accepted as much as possible.
- Power injection in one bus node is limited and the bus voltage should always be within an allowable range during the real time control.
- Real-time data need to be compared with predicted data for PV output power, electricity demand of a building, available PEV and current status, SOC of battery storage.

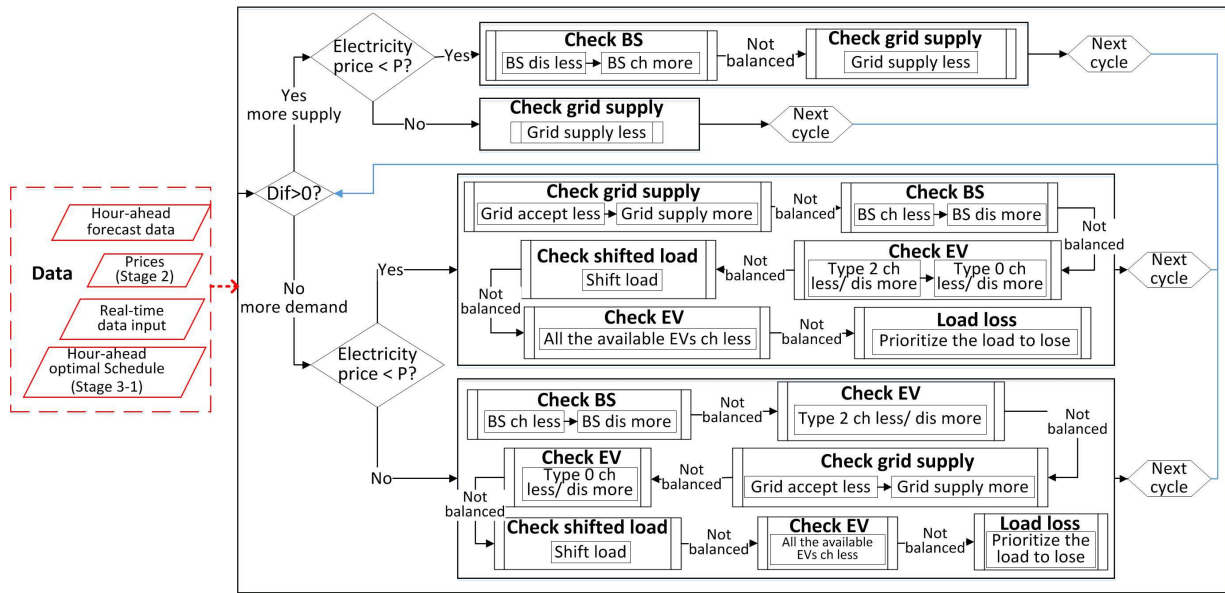


Fig. 4. Flowchart of the control strategy.

- EVs are classified into three groups according to their charging demand and departure time: 1) must participate at this time slot to meet the demand, 2) can be flexible load, 3) the same as predicted, and thus remain the same as scheduled. If a certain PEV is not scheduled for charging in this time slot in the hour-ahead schedules, the real-time control will not change the schedule unless necessary.
- Different scenarios are separated, where the checking logic and priorities are defined for each scenario.
- When more power is supplied than predicted, reduce power supply from main grid if real time electricity price is high, while reduce power supply from battery storage or restore the extra power to battery storage if real time electricity price is low.
- When the power demand at real time is more than the predicted power demand,
 - Increase the power supply from battery storage first if real time electricity price is high; Increase the power supply from main grid first if price is low.
 - If battery storage and main grid cannot balance the extra demand, the charging/discharging schedules of group 2 PEVs can be adjusted.
 - The schedules of group 3 PEVs can be adjusted if the power is still not balanced.
 - Type 3 load can be shifted to later time slots if load demand change is necessary.
 - If load loss is inevitable, the priorities are based on the cost of energy not supplied indices for each load type.
 - The control scheme reserves power in case some large deviations with predicted data occur.

In fact, the real situation of the PEVs coming to the charging station is highly uncertain, thus it is pretty possible that the scheduled PEVs in the prediction are not coming, more PEVs come than predicted, scheduled PEVs come later or earlier,

Algorithm 1 Real Time Control Strategy

load : hour-ahead optimal solution
input : hour-ahead forecast data, real time b_b^t, p_{PV}^t
output : real time scheduling of $P_G^{t+}, P_G^{t-}, e_i^{t+}, e_i^{t-}, s_{BS}^{t+}, s_{BS}^{t-}$

1. **update** t , **input**
2. initiate real time scheduling by hour-ahead optimal solution
3. classify existing EVs and check Dif
4. **if** $Dif > 0$
 Check example:

$$\text{if } \sigma < \sigma_{lim} \rightarrow \text{if } \begin{cases} p_{BS}^t + s_{BS}^{t+} - s_{BS}^{t-} + Dif > s_{BS}^{max,c} \\ \text{or } Dif > r_{BS}^{avl,c} \text{ or } Dif > r_{BS}^c - s_{BS}^{t+} \end{cases} \rightarrow \begin{cases} \Delta s_{BS}^{t+} = \min(s_{BS}^{avl,c}, s_{BS}^{max,c} - (p_{BS}^t + s_{BS}^{t+} - s_{BS}^{t-})) \\ \Delta P_G^{t-} = Dif - \Delta s_{BS}^{t+} \end{cases}$$
 else $\rightarrow \Delta s_{BS}^{t+} = Dif$
 else $\rightarrow \Delta P_G^{t-} = Dif$
5. **elseif** $Dif < 0$, **check** ...
6. **jump to 1** until next hour
7. **end**

or status of the battery is very different from predicted data, etc. All the above-mentioned scenarios are considered in the control scheme to best match the real situation. The algorithm is briefly presented as Algorithm 1.

D. Comparison With the Basic Control Scheme

The basic control scheme does not consider the priority criteria in the proposed control scheme. The basic control is needed in real time due to the inevitable existence of the difference between predicted value and real data. The charging station always tries to store extra energy to the fixed battery storage first and supply extra demand from the main grid to meet the charging/ discharging efficiency of the battery.

To evaluate the validity of the proposed algorithm, the comparison is carried out to show the benefits of having the stage II, stage III and stage IV, respectively. Thus, results

TABLE I
COMPARISON RESULTS AND ANALYSIS

Evaluate	Section: Case vs.	Observation	Conclusion
Stage III: Hour-ahead schedules	IV-A: Day-ahead schedule (case 1) vs. Hour-ahead schedule (case 2)	<ul style="list-style-type: none"> In case 2, battery storage stored more energy during low electricity price hours 2-7, which saved more cost during hours 10-15 (there is a quite large deviation of PV output power from hour 10-15 in Fig. 5). In case 1, few deferrable loads supplied during high electricity price hours 8-11 gave load burden to later hours. The situation became worse due to the unforeseen output power deviation from PVs. The impact is accumulated with time causing significant load burden for the last several hours. The overall cost in case 1 is 15 times of case 2. 	It can be concluded that using hour-ahead forecast data in the optimization model is better.
Stage IV: Real-time control	IV-B: Hour-ahead schedule (case 2) vs. Real-time control (case 3)	<ul style="list-style-type: none"> The change of battery storage SOC seems quite similar except more discharge is scheduled in hour 10 (case 3). Due to different initial SOC of battery storage, deferrable load in hour 11 for case 3 is less than in case 2. PEV charging/discharging schedules are different in several time slots, but the overall PEV consumption is the same. There is a significantly higher cost at the end of day for case 2, and the overall cost of case 2 is 1.55 times of case 3. In case 3, more power supply is accepted from grid in several time slots even though the electricity price is not low. It may cause the overall cost to increase more or less if predicted data is quite accurate, but it will save a lot of cost if some unpredictable conditions happen, e.g. the case discussed in this paper. 	<ul style="list-style-type: none"> The proposed control scheme is more prepared for unfavorable conditions. Load profile is not simply flattened as in the traditional demand response since the grid is not the only source of power. PV generation, fixed energy storage and PEV mobile energy storage are integrated in the network, which makes it hard to intuitively predict the optimal solution for the overall operation. The target is to reduce the operational cost for the integrated charging station.
Extended coverage time	IV-C: 24h (case 4) vs. extended coverage (case 1)	<ul style="list-style-type: none"> The load loss happens in both cases, causing high cost due to the customer satisfaction related indices being low in the cost function. More deferrable load is supplied during high electricity price hours and the utilization ratio of the fixed battery storage is higher in case 1. Case 4 has more load loss and overall cost is about 1.4 times of case 1. 	The use of extended coverage hours gives higher tolerability and flexibility for unpredictable circumstances.
Stage II: Price update	IV-D: Stage I vs. Stage II price	The costs with Stage II price are higher than those with Stage I price, but the differences are small enough to be neglected.	It is beneficial to update prices since higher bonus can attract more PEV customers to park and charge there.
Stage I&III: Chance- constrained optimization	IV-E: None vs. Base case vs. More reliable case	<ul style="list-style-type: none"> More energy is reserved in the fixed battery storage when Rei is higher (more reliable) in case a fault happens. More reliable case tends to have less cost induced by the energy not supplied when fault happens. The cost due to the energy not supplied during fault is very low during hours 5-14, since the PV generation is quite active during those hours. 	The adoption of chance-constrained optimization will lead to lower loss especially when the fault happens.

of using stage I and stage II electricity prices and participation bonus, results from using day-ahead forecast data and hour-ahead forecast data, and results of using the basic control scheme vs. the proposed control scheme are compared. Also, the results of using 24 hours as a cycle vs. flexible hours based on the last departure PEV are compared.

III. SIMULATION AND CASE STUDY RESULTS

According to the day-ahead forecast data for PEVs, 29 hours are covered in each hour-ahead simulation. The predicted output power from solar panels as shown in Fig. 5 is based on [30]. Operational cost for PV and fixed battery storage are assumed based on [31] and [32]. The capacity of the fixed battery storage is assumed to be 113.4 kWh and maximum charging/discharging rate is 70.875 kW/hour. The maximum output power of PV is assigned to be 153 kW. 18 chargers are assumed to be installed in the charging station, so no more than 18 PEVs can be connected and exchange power at the same time. The charging rate for each charger is set at 7.2 kW/h. The target area is assumed to have a population of 300 with the PEV penetration of 30%. In this simulation, the building and the integrated charging station including PV generation, EV chargers and fixed battery storage are connected to the same bus. The whole integrated system in Fig. 1 is connected to bus 18 in IEEE 33 bus test distribution system [33]. The case studies are explained below. Summary observations and conclusion for each comparison are elaborated in Table I.

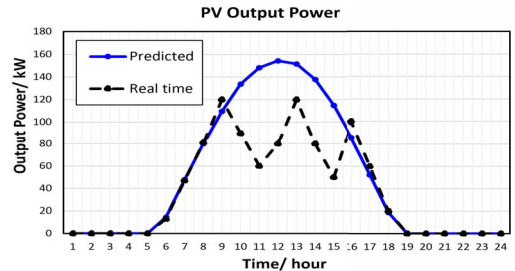


Fig. 5. Predicted Output Power from PV.

A. Day-Ahead Schedule vs. Hour-Ahead Schedule

This comparison shows whether the cost will be decreased if hour-ahead schedules instead of day-ahead schedules are used. Obviously, hour-ahead forecast is more accurate. However, in the proposed algorithm, it is possible that using hour-ahead data may cause higher cost. Optimization for hour-ahead schedules need to be implemented every hour and up to 29 hours are covered in each simulation. Since the deferrable load in hour 1-24 may be shifted to hour 25-29, the shifted load need to be compensated at later hours to guarantee all the deferrable load (1-24) are supplied within a day (24 hours). Each hour-ahead simulation may output different schedules for the deferrable load supply. Thus, even though the hour-ahead schedules may give more optimized schedule for the current time slot, it may induce more burden to later hours. Therefore,

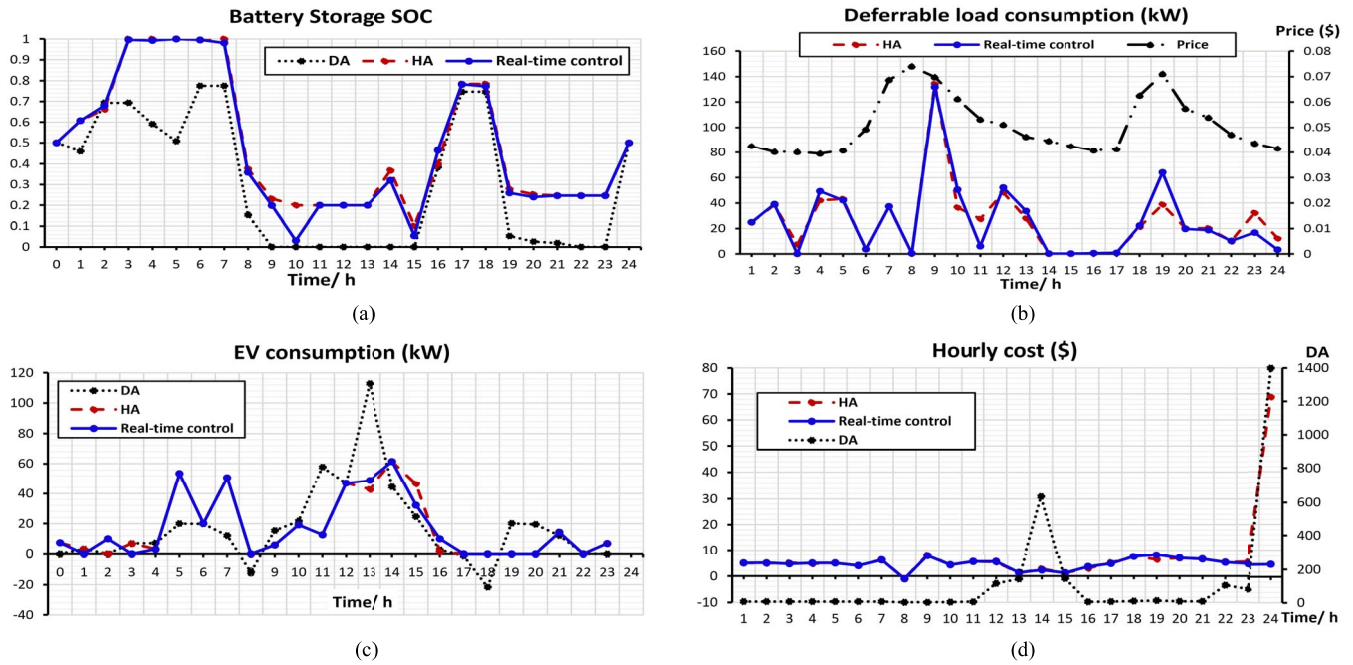


Fig. 6. DA vs. HA vs. real-time (a) Battery storage SOC comparison (b) Deferrable load consumption comparison (c) PEV consumption comparison (d) Hourly cost comparison.

it is still meaningful to compare the results of using day-ahead and hour-ahead schedules. The comparison results of battery storage SOC, deferrable load consumption, PEV consumption, and hourly cost, are shown in Fig. 6.

B. Hour-Ahead Schedule vs. Real-Time Control

This comparison shows whether the results will be improved if the proposed control scheme is used, as shown in Fig. 6. In this study, a relatively unfavorable situation is assumed where the PV output power is not quite as predicted, especially during low electricity price hours when the load schedule is supposed to be higher. This scenario is reasonable since in real life PV output power can be fairly uncertain and flexible as sunlight changes.

C. Coverage Time of 24h vs. the Departure of the Last PEV

This comparison shows whether covering the individual connection time intervals of all the arrived PEVs is better than a fixed 24 hours. It should be pointed out that even though the coverage time in the simulation is extended, the control cycle of a day always starts at midnight and ends at the next midnight. The reason of extending the simulation coverage time is that splitting the connection time of PEVs into two days is not desired, and assigning a new target SOC at the end of a day will limit the optimization results. For example, a PEV may arrive at 10 pm with an initial SOC of A and may leave at 5 am the next day with the target SOC of B. If it is the last car to leave the charging station, the coverage time in the simulation will be 29 hours. If the coverage time is set to be always 24 hours, it is necessary to assign a temporary target SOC at the end of the first day, which will narrow the feasible region of the optimization model. Extending the coverage

time may bring more uncertainties since the deferrable load that are scheduled to be shifted to extended hours (25-29) need to also be reflected within 24 hours. Making the comparison is still necessary. To simplify the simulation, we use case 1 in Section II-A to represent the use of extended coverage time, and use the coverage time of 24 hours in the same model. The comparison results of deferrable load consumption, fixed battery storage SOC, and hourly cost are shown in Fig. 7.

D. Stage I Prices vs. Stage II Prices

This comparison demonstrates whether using the updated prices from stage II will cause any negative impact on the cost. In the proposed algorithm, PEV charging prices and discharging participation bonus vary with time and are based on the load profile. The load consumption will change after the day-ahead predictions give new building consumption schedules and PEV charging/ discharging schedules. In order to provide more incentives to PEV customers, the discharge bonus is maximized. Larger bonus value will lead to higher cost for the charging station, so a maximum cost limit C is guaranteed as a constraint. Undoubtedly, if the updated bonus value in stage II is much higher than original value in stage I, the cost will be increased accordingly when discharging is needed. As a tradeoff, it will lower the priority of discharging PEVs when extra supply is needed. The comparison results of the hourly cost from case 1 to case 4 are shown in Fig. 8.

E. The Effect of the Chance-Constrained Optimization

The effect of adopting chance-constrained optimization can be observed when the fault happens. Three cases are generated: 1) no chance-constrained optimization; 2) base case: R_{ei} in (17) is set to be 0.97; and 3) more reliable: R_{ei} is set

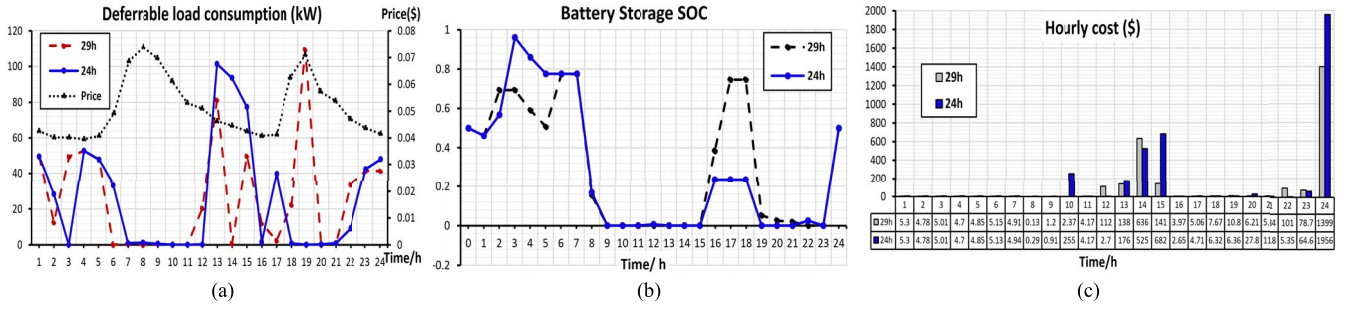


Fig. 7. 29h vs. 24h (a) Deferrable load consumption comparison (b) Battery storage SOC comparison (c) Hourly cost comparison.

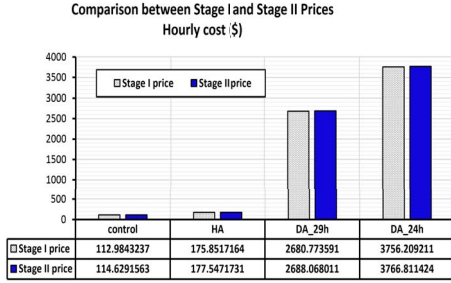


Fig. 8. Hourly cost comparison between stage I price and stage II price.

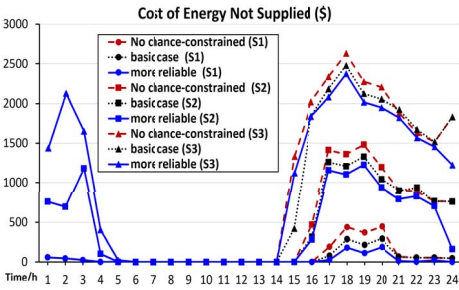


Fig. 9. Cost of energy not supplied under different cases and scenarios.

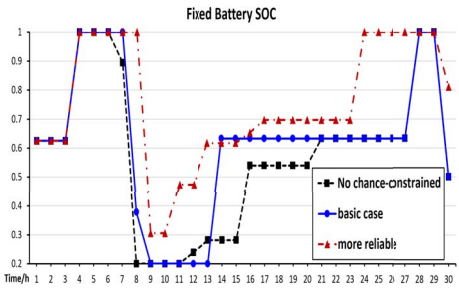


Fig. 10. Fixed battery SOC under different cases time in real time control.

to be 0.99. We assume that when the fault happens, the grid won't be able to provide any energy. The probability of the fault occurrence is 0.95. Three scenarios are considered under each case: S1- fault lasts for 1 hour, S2- fault lasts for 2 hours; and S3- fault lasts for 3 hours. The cost of the energy not supplied and fixed battery SOC when the fault happens at different hours in a day under different scenarios and cases are illustrated in Fig. 9 and 10.

F. Computational Efficiency Analysis

Computational efficiency is a requirement for simulations. As discussed in Section II-B, the optimization model is solved as DC system in this paper to save more computational time. The computational time for hour-ahead optimization in stage III is about 16.931227 seconds on a computer with quad core processor (1.6 GHz Intel i5) and 8 GB RAM. It takes another 0.013601 seconds to run the simulation to obtain the estimated real time data from the most recent real-time control for hour-ahead optimization. In the case study, the hour-ahead optimization is implemented 15 minutes before each hour. But the computational time allows the gap to be as short as 30 seconds before each hour, to leave some redundancy. For the real time control, each simulation takes about 0.034030 seconds on a computer with dual core processor (2 GHz Intel i5) and 8 GB RAM, including extracting real time data as input. The value may change for each simulation, but the difference remains within 0.02 seconds. Compared with the algorithm in [22] with a computational complexity of $O(T^3)$ and computational time of the range 1-10 seconds, the proposed control algorithm is pretty fast. In this case study, the real-time control is implemented every 15 minutes, but it can be easily adjusted to shorter intervals. The computational time allows the real time control to be implemented for each second. Note that the computational time is based on the operational speed of individual computers. In conclusion, the control algorithm is pretty computationally efficient.

The results of the proposed four-stage algorithm are compared with the results of directly applying the proposed optimization model in real time which will make the solution more optimal. The comparison results indicate that the performance gap of the total cost is smaller than 0.4%, but the proposed four-stage algorithm saved a lot more computational time in real time control.

IV. CONCLUSION

In this paper, a four-stage optimization and control algorithm is proposed for the purpose of reducing the operational cost of the integrated smart charging station. The proposed algorithm spans three time scales, has an additional stage II to deal with PEV charging/discharging prices to attract customers to participate, and offers a novel control scheme design to

improve the operational performance. The following are some major findings:

- By using the extended coverage hours, no temporary parameter needs to be assigned, and also the integrated station is more prepared for unpredictable condition.
- It is beneficial for both PEV customers and charging station owners to use updated PEV charging price and discharging program participation bonus in Stage II.
- Using the hour-ahead forecast data to optimize the schedules will not only provide more accurate data, but also dramatically decrease the overall cost.
- The proposed control scheme provides higher tolerability for unpredictable circumstances.

This algorithm can easily be applied to integrated charging stations connected to any other types of building by replacing the predicted load profile, consumption percentage of each load type and predicted PEV consumption (probability distribution of arriving time) as needed.

REFERENCES

- [1] X. E. Yu, Y. Xue, S. Siroospour, and A. Emadi, "Microgrid and transportation electrification: A review," in *Proc. IEEE Transp. Electrification Conf. Expo (ITEC)*, Dearborn, MI, USA, 2012, pp. 1–6.
- [2] P. Kou, D. Liang, L. Gao, and F. Gao, "Stochastic coordination of plug-in electric vehicles and wind turbines in microgrid: A model predictive control approach," *IEEE Trans. Smart Grid*, vol. 7, no. 3, pp. 1537–1551, May 2016.
- [3] Q. Yan, B. Zhang, and M. Kezunovic, "The demand response support under weather impacts using PV generation and EV energy storage," in *Proc. IEEE 16th Int. Conf. Environ. Elect. Eng. (EEEIC)*, Florence, Italy, 2016, pp. 1–6.
- [4] J. V. Roy *et al.*, "Electric vehicle charging in an office building microgrid with distributed energy resources," *IEEE Trans. Sustain. Energy*, vol. 5, no. 4, pp. 1389–1396, Oct. 2014.
- [5] H. K. Nguyen and J. B. Song, "Optimal charging and discharging for multiple PHEVs with demand side management in vehicle-to-building," *J. Commun. Netw.*, vol. 14, no. 6, pp. 662–671, Dec. 2012.
- [6] C. Marmaras, M. Corsaro, E. Xydias, L. M. Cipcigan, and M. A. Pastorelli, "Vehicle-to-building control approach for EV charging," in *Proc. 49th Int. Univ. Power Eng. Conf. (UPEC)*, Cluj-Napoca, Romania, 2014, pp. 1–6.
- [7] G. Cardoso *et al.*, "Stochastic programming of vehicle to building interactions with uncertainty in PEVs driving for a medium office building," in *Proc. 39th Annu. Conf. IEEE Ind. Electron. Soc. (IECON)*, Vienna, Austria, 2013, pp. 7648–7653.
- [8] S. Rezaee, E. Farjah, and B. Khorramdel, "Probabilistic analysis of plug-in electric vehicles impact on electrical grid through homes and parking lots," *IEEE Trans. Sustain. Energy*, vol. 4, no. 4, pp. 1024–1033, Oct. 2013.
- [9] F. Sun, W. Hou, B. Yin, and H. Xi, "Preliminary studies on the linking of building hybrid energy system and distributed power generation system," in *Proc. Int. Conf. Sustain. Power Gener. Supply*, Nanjing, China, 2009, pp. 1–6.
- [10] H. Huang, Y. Cai, H. Xu, and H. Yu, "A multiagent minority-game-based demand-response management of smart buildings toward peak load reduction," *IEEE Trans. Comput.-Aided Design Integr. Circuits Syst.*, vol. 36, no. 4, pp. 573–585, Apr. 2017.
- [11] Y.-M. Wi, J.-U. Lee, and S.-K. Joo, "Electric vehicle charging method for smart homes/buildings with a photovoltaic system," *IEEE Trans. Consum. Electron.*, vol. 59, no. 2, pp. 323–328, May 2013.
- [12] W. Su, J. Wang, and J. Roh, "Stochastic energy scheduling in microgrids with intermittent renewable energy resources," *IEEE Trans. Smart Grid*, vol. 5, no. 4, pp. 1876–1883, Jul. 2014.
- [13] Y. Guo, J. Xiong, S. Xu, and W. Su, "Two-stage economic operation of microgrid-like electric vehicle parking deck," in *Proc. IEEE/PES Transm. Distrib. Conf. Expo. (T D)*, Dallas, TX, USA, 2016, p. 1.
- [14] W. Tushar, C. Yuen, S. Huang, D. B. Smith, and H. V. Poor, "Cost minimization of charging stations with photovoltaics: An approach with EV classification," *IEEE Trans. Intell. Transp. Syst.*, vol. 17, no. 1, pp. 156–169, Jan. 2016.
- [15] C. Chen, S. Duan, T. Cai, B. Liu, and G. Hu, "Smart energy management system for optimal microgrid economic operation," *IET Renew. Power Gener.*, vol. 5, no. 3, pp. 258–267, May 2011.
- [16] M. Montoya, R. Sherick, P. Haralson, R. Neal, and R. Yinger, "Islands in the storm: Integrating microgrids into the larger grid," *IEEE Power Energy Mag.*, vol. 11, no. 4, pp. 33–39, Jul./Aug. 2013.
- [17] B. Washom *et al.*, "Ivory tower of power: Microgrid implementation at the university of California, San Diego," *IEEE Power Energy Mag.*, vol. 11, no. 4, pp. 28–32, Jul./Aug. 2013.
- [18] Q. Xu *et al.*, "Day-ahead battery scheduling in microgrid considering wind power uncertainty using ordinal optimization," in *Proc. North Amer. Power Symp. (NAPS)*, Pullman, WA, USA, 2014, pp. 1–6.
- [19] G. C. Liao, "The optimal economic dispatch of smart microgrid including distributed generation," in *Proc. Int. Symp. Next Gener. Electron.*, Kaohsiung, Taiwan, 2013, pp. 473–477.
- [20] M. Zhang and J. Chen, "The energy management and optimized operation of electric vehicles based on microgrid," *IEEE Trans. Power Del.*, vol. 29, no. 3, pp. 1427–1435, Jun. 2014.
- [21] H. Nafisi, S. M. M. Agah, H. A. Abyaneh, and M. Abedi, "Two-stage optimization method for energy loss minimization in microgrid based on smart power management scheme of PHEVs," *IEEE Trans. Smart Grid*, vol. 7, no. 3, pp. 1268–1276, May 2016.
- [22] W. Tang and Y. J. Zhang, "A model predictive control approach for low-complexity electric vehicle charging scheduling: Optimality and scalability," *IEEE Trans. Power Syst.*, vol. 32, no. 2, pp. 1050–1063, Mar. 2017.
- [23] Q. Yan, I. Manickam, M. Kezunovic, and L. Xie, "A multi-tiered real-time pricing algorithm for electric vehicle charging stations," in *Proc. IEEE Transp. Electrification Conf. Expo (ITEC)*, Dearborn, MI, USA, 2014, pp. 1–6.
- [24] Q. Yan, C. Qian, B. Zhang, and M. Kezunovic, "Statistical analysis and modeling of plug-in electric vehicle charging demand in distribution systems," in *Proc. Int. Conf. Intell. Syst. Appl. Power (ISAP)*, San Antonio, TX, USA, 2017, pp. 1–6.
- [25] N. U. Hassan, Y. I. Khalid, C. Yuen, and W. Tushar, "Customer engagement plans for peak load reduction in residential smart grids," *IEEE Trans. Smart Grid*, vol. 6, no. 6, pp. 3029–3041, Nov. 2015.
- [26] *Reload Database Documentation and Evaluation and Use in NEMS*. Accessed: Jul. 13, 2017. [Online]. Available: <http://www.onlocationinc.com>
- [27] J. K. Gruber and M. Prodanovic, "Two-stage optimization for building energy management," *Energy Procedia*, vol. 62, pp. 346–354, Dec. 2014.
- [28] *New Hampshire Electric Co-op Load Profiles*. Accessed: Jul. 13, 2017. [Online]. Available: <https://www.nhec.com/electric-choice/load-profiles/>
- [29] Q. Yan, T. Dokić, and M. Kezunovic, "Predicting impact of weather caused blackouts on electricity customers based on risk assessment," in *Proc. IEEE Power Energy Soc. Gen. Meeting (PESGM)*, Boston, MA, USA, 2016, pp. 1–5.
- [30] *California Irrigation Management Information System (CIMIS)*. Accessed: Jul. 13, 2017. [Online]. Available: <http://www.cimis.water.ca.gov/>
- [31] *Distributed Generation Renewable Energy Estimate of Costs*, Nat. Renew. Energy Lab., Golden, CO, USA, 2016. [Online]. Available: <http://www.nrel.gov/analysis/>
- [32] *Energy Storage Study 2014*, California Energy Commission, Sacramento, CA, USA, 2014. [Online]. Available: http://energy.ca.gov/assessments/ab2514_reports
- [33] *IEEE 33-Bus Test Distribution System*. Accessed: Jul. 13, 2017. [Online]. Available: <https://www.scribd.com/doc/143306826/IEEE-33-Bus-Test-Distribution-System>



Qin Yan (S'12) received the B.S. degree in electrical engineering from Wuhan University, China, in 2010 and the M.Eng. degree from Texas A&M University, College Station, in 2012, where she is currently pursuing the Ph.D. degree.

Her research interests include plug-in electric vehicles, smart grid, distributed energy resources, and optimization algorithms.



Bei Zhang (S'12) received the B.S. and M.S. degrees from Shanghai Jiao Tong University, Shanghai, China, in 2009 and 2012, respectively, and the Ph.D. degree in electrical engineering from Texas A&M University in 2017. She is currently with GE Power, Schenectady, NY, USA.

Her research interests include power system reliability, electric vehicle, and electricity market.



Mladen Kezunovic (S'77–M'80–SM'85–F'99–LF'17) received the Dipl.Ing., M.S., and Ph.D. degrees in electrical engineering in 1974, 1977, and 1980, respectively. He has been with Texas A&M University for 31 years.

He is currently a Regents Professor, an Eugene E. Webb Professor, the Director of the Smart Grid Center, and the Site Director of Power Engineering Research Center, PSerc consortium. His expertise is in protective relaying, automated power system disturbance analysis, computational intelligence, data analytics, and smart grids. He has published over 550 papers, given over 120 seminars, invited lectures and short courses, and consulted for over 50 companies worldwide. He is the Principal of XpertPower Associates, a consulting firm specializing in power systems data analytics.

Dr. Kezunovic is a CIGRE Fellow, a Honorary Member, and a Registered Professional Engineer in TX, USA.